



INSTITUT DE FRANCE
Académie des sciences

Comptes Rendus

Chimie

Sana Jmai, Sami Guiza, Salah Jellali, Mohamed Bagane and Mejdì Jeguirim

Competitive bio-sorption of basic dyes onto petiole palm tree wastes in single and binary systems

Volume 25, Special Issue S2 (2022), p. 27-41

Published online: 25 February 2022

<https://doi.org/10.5802/crchim.155>

Part of Special Issue: Sustainable Biomass Resources for Environmental, Agronomic, Biomaterials and Energy Applications 3

Guest editors: Mejdì Jeguirim (Université de Haute-Alsace, Institut de Sciences des Matériaux de Mulhouse, France), Salah Jellali (Sultan Qaboos University, Oman) and Besma Khiari (Centre of Water Researches and Technologies, Tunisia)



This article is licensed under the
CREATIVE COMMONS ATTRIBUTION 4.0 INTERNATIONAL LICENSE.
<http://creativecommons.org/licenses/by/4.0/>



Les Comptes Rendus. Chimie sont membres du
Centre Mersenne pour l'édition scientifique ouverte
www.centre-mersenne.org
e-ISSN : 1878-1543



Sustainable Biomass Resources for Environmental, Agronomic, Biomaterials and Energy Applications 3 / *Ressources de biomasse durables pour des applications environnementales, agronomiques, de biomatériaux et énergétiques 3*

Competitive bio-sorption of basic dyes onto petiole palm tree wastes in single and binary systems

Biosorption compétitive des colorants basiques sur des déchets de pétiole de palmier dans les systèmes simples et binaires

Sana Jmai^{® a}, Sami Guiza^{® *, a}, Salah Jellali^{® b}, Mohamed Bagane^{® a}
and Mejdi Jeguirim^{® c}

^a Department of Chemical Engineering Process, National Engineering School of Gabes, University of Gabes, Tunisia

^b Center for Environmental Studies and Research, Sultan Qaboos University, Al-Khoud 123, Oman

^c Université de Haute-Alsace Institut de Sciences des Matériaux de Mulhouse 3 rue Alfred Werner 68093 Mulhouse, France

E-mails: sanajmai1@gmail.com (S. Jmai), sami_guiza@yahoo.fr (S. Guiza), s.jellali@squ.edu.om (S. Jellali), drmbag1420@yahoo.fr (M. Bagane), mejdi.jeguirim@uha.fr (M. Jeguirim)

Abstract. This work aimed to study petiole palm tree wastes (PTW) efficiency in removing two basic dyes: Rhodamine B (RB) and Victoria blue B (VBB) from aqueous solutions in single and binary systems under various experimental conditions including the effect of contact time, pH, initial concentration, and temperature. The PTW characterization shows that the PTW is a lingo-cellulosic material. The experimental results indicate that the removal of both dyes was relatively fast, spontaneous, exothermic and occurred on monolayers. Moreover, the adsorption competition between these two dyes on the adsorbent particles surface was important since the Langmuir's adsorption capacities were evaluated to 260.1; 440.1; 168.0; and 417.4 mg/g for RB and VBB in single and binary systems, respectively. These adsorption capacities, even in binary systems, are interesting compared to other raw materials and prove that this abundant agricultural waste can be considered as a promising material for an efficient dyes removal from aqueous effluents.

Résumé. Ce travail vise à étudier l'efficacité des déchets de pétiole de palmier (PTW) pour l'élimination de deux colorants basiques : la Rhodamine B (RB) et le Victoria bleu B (VBB) en solution aqueuse pour des systèmes simples et binaires dans diverses conditions expérimentales, y compris l'effet du temps de contact, le pH, la concentration initiale et la température. La caractérisation du PTW montre

* Corresponding author.

que ce dernier est un matériau ligno-cellulosique. Les résultats expérimentaux indiquent que l'élimination des deux colorants était relativement rapide, spontanée, exothermique et se produisait sur des monocouches. De plus, l'adsorption compétitive entre ces deux colorants basiques à la surface des particules PTW était importante puisque les capacités d'adsorption d'après le model de Langmuir ont été évaluées à 260.1 ; 440.1 ; 168.0 et 417.4 mg/g pour le RB et le VBB dans les systèmes simples et binaires, respectivement. Ces capacités d'adsorption, même en systèmes binaires, sont intéressantes par rapport à d'autres matières premières et prouvent que ces déchets agricoles abondants peuvent être considérés comme matériau prometteur pour une décoloration efficace des effluents aqueux.

Keywords. Petiole palm tree wastes, Dyes, Competition, Adsorption, Characteristics, Modeling.

Mots-clés. Déchets de pétiole de palmier, Colorants, Compétitive, Adsorption, Caractérisation, Modélisation.

Published online: 25 February 2022

1. Introduction

Contaminated effluents discharged by textile, paper, plastics, and dye industries are the main sources of aquatic pollution [1]. These industries generally generate huge amounts of wastewaters that contain mixture of organic and inorganic chemicals that potentially threat the environment quality [2,3] as well as public health [4,5]. For this reason, the treatment of these effluents has been identified as a global environmental concern. Color, which is mainly due to the presence of dyes, is one of the first aspects to be inspected when dealing with wastewater [6]. Even in small quantities (less than 1 ppm for some of them), dyes can be easily detected [7], and potentially toxic to humans and animals [8]. The RB and VBB, as cationic dyes, are widely used as coloring agents in several industries [9]. Their efficient removal from aqueous solutions is therefore a critical issue that has to be seriously taken into consideration.

Many techniques have been suggested for the removal and separation of dyes from contaminated waters, including photo-degradation [10] coagulation [11], electro-oxidation [12–14], and membrane filtration [15]. The real implementation of these technologies is generally hindered by several drawbacks including high capital and exploitation costs, sensitive operational conditions, use of large amounts of chemicals, and the presence of a secondary sludge or byproducts that have to be additionally treated [16].

Adsorption [17,18] has been identified, these last decades, as an attractive method, liable to be used separately or in combination with other technologies for efficient dyes removal from aqueous solutions [19]. The main advantages of adsorption compared to other technologies are simplicity, low cost, and efficiency [20].

Several organic and inorganic adsorbents such as clays [21,22], activated carbon [23,24], cellulose [25–27], carbon nano-tubes [28], magnetic composites [29], bio-composite [30,31], bio-wastes [32–34], industrial by-products, and natural materials such biopolymers, have been utilized in dye removal [35,36]. The use of raw agricultural materials, without any modification, is however highly recommended in order to limit the treatment cost.

In Tunisia, date palm oases generated huge amounts of biomass that can be valorized as a low cost material for wastewater treatment in general and dyes removal in particular. Indeed, more than 4.3 million date palm trees exist in the southern part of Tunisia occupying an area of almost 42,000 ha [37]. Nowadays, there is no specific management option of the produced wastes in these oases. Indeed, the majority of these biomasses are generally thrown away or openly burned raw which induces serious environmental risks.

Date palm wastes have been applied as raw materials for the removal of both organic and inorganic pollutants from wastewaters [38]. Other studies have focused on the synthesis of activated carbons from these wastes and their application for the removal of a wide range of pollutants such as chromium, phenol, methylene blue etc... [39–42]. However, the majority of these studies investigated the behavior of a single contaminant without an important accent on the involved mechanisms. Moreover, RB and VB removal studies are relatively rare compared to other common dyes such as methylene blue and methyl orange. Specific studies dealing with the impact of the presence of mixed dissolved dyes on their removal efficiency from effluents are of great interest.

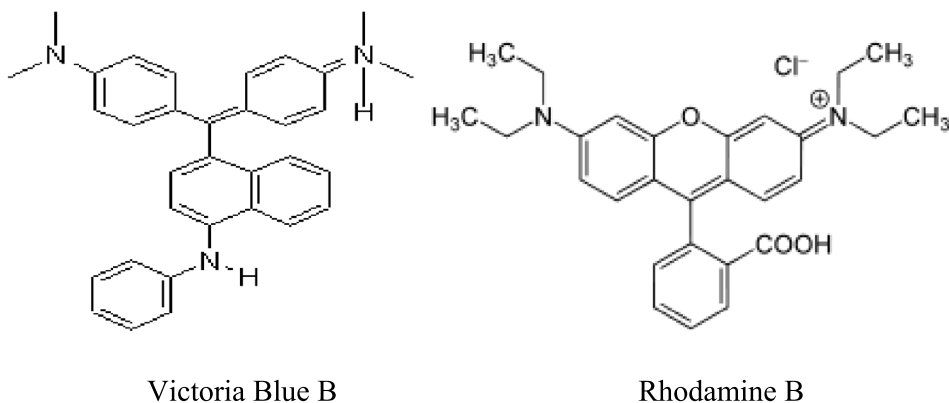


Figure 1. VBB and RB chemical structures.

The present work mainly aims to highlight the effect of the competition process between RB and VB on their removal from aqueous solutions by an abundant biomass (petiole palm tree wastes). For this aim, these two basic dyes removal efficiency from aqueous solutions was precisely assessed in single and binary systems under various experimental conditions such as contact time, pH, initial concentration, adsorbent dose, and temperature. The involved mechanisms were explored through kinetic and isotherm modeling as well as Fourier Transform Infrared (FTIR) analyses.

2. Materials and methods

2.1. Adsorbent preparation and characterization

The petiole palm tree waste used in this study was collected from the region of Gabes, southern region of Tunisia. It was ground and sieved in order to obtain a homogenous particles distribution. The mean size of the material is 250 μm . The obtained raw material was not subjected to any form of pretreatment before its use as an adsorbent for dyes removal from aqueous solutions.

The preliminary raw material characterization has targeted the determination of its zero-point charge pH (pH_{PZC}), at this point the surface charge of the adsorbent was neutral. This parameter was determined according to the approach given by Hammani *et al.* [43] for initial pH varying from 2 to 12. Besides the main functional groups of this adsorbent was performed through Fourier transform infra-red

(FTIR) spectroscopy using a Brunker-tensor 27 spectrometer.

2.2. Dye solution preparation and analysis

Rhodamine B (chemical formula (CF): $\text{C}_{28}\text{H}_{31}\text{ClN}_2\text{O}_3$; molar weight (MW) = $479.01 \text{ g}\cdot\text{mol}^{-1}$) and Victoria blue B (CF: $\text{C}_{33}\text{H}_{32}\text{ClN}_3$; MW = $506.09 \text{ g}\cdot\text{mol}^{-1}$), used in this study for the preparation of the synthetic solutions, were purchased from Acros-Organics from (USA). Their molecular structures are represented in Figure 1. These dyes were used as supplied, without any prior purification.

During the adsorption tests, two stock solutions of RB and VBB of $1000 \text{ mg}\cdot\text{L}^{-1}$ were prepared and used for solutions preparation at desired concentrations. The efficiency of the adsorbent in removing RB and VBB under the different experimental conditions was determined through the assessment of their absorbance at wavelength values of 553.2 and 614.5 nm, respectively, using an UV spectrophotometer (Genesys 10S UV-Vis).

2.3. Adsorption experiments

RB and VBB adsorption experiments were conducted in a 2 L batch reactor provided with a water circulation arrangement to maintain the temperature at the desired value [44]. These experiments consisted in mixing given masses of the adsorbent in 1 L of synthetic solution containing these dyes at a desired concentration in single or binary modes for a fixed contact time. These mixtures were stirred with an

electromagnetic stirrer (Kika-Werke-RT 10 Power) at a constant speed of 200 rpm. The remaining dissolved RB or VBB concentrations were determined using the above cited UV–visible spectroscopy apparatus after centrifugation at 2000 rpm for 5 min with a CENTROMIX mod S-549 apparatus.

All these assays were performed in triplicate and the mean values were reported in this study. The standard deviation for all assays was lower than 5%.

2.3.1. Effect of initial pH

The influence of the pH on the adsorption of a series of colored solutions at 20 mg·L⁻¹ in RB and VBB was monitored. The pH of the solutions was adjusted to values ranging from 3 to 8 since the behavior of the VBB used is considerably dependent on the pH of the water: at pH < 8, it is blue in color, but at pH > 8 it acquires a red color. The pH of the solutions has been adjusted by adding a few drops of HCl (0.1 N) or NaOH (0.1 N) solutions and the adsorbent dose used was fixed at 0.1 g/L. The mixtures were then stirred at 200 rpm for 3 h at room temperature 25 °C. The residual dye concentrations were determined by the spectrophotometer analysis.

2.3.2. Effect of contact time- kinetic study

The kinetic adsorption of RB and VBB by the raw PTW biomass in single and binary modes was assessed at times ranging between 5 and 120 min. These assays were carried out for initial dye concentrations ranging between 10 and 50 mg·L⁻¹ in single mode and from 6 to 14 mg·L⁻¹ in binary mode, a constant adsorbent dosage of 0.1 g·L⁻¹, and a fixed pH of 4 for both RB and VBB. The RB or VBB adsorbed amounts at a given time “*t*”, (*q_t*) (1) and the corresponding removal yield (*Y_t*) (2) were assessed as follows:

$$q_t = \frac{(C_0 - C_t)}{D} \quad (1)$$

$$Y_t(\%) = \frac{(C_0 - C_t)}{C_0} \times 100 \quad (2)$$

where *C₀* and *C_t* (mg·L⁻¹) are the dye concentrations at the beginning of the experiment and at a given time “*t*”, respectively, and *D* is the used PTW dose (g·L⁻¹).

The RB and VBB adsorption kinetics measured data were fitted to three well-known models (Table 1), namely pseudo-first order (PFO), pseudo-second order (PSO), and Elovich. The original and the

linearized equations of these four models are extensively cited in literature [45,46].

Table 1. Used kinetics models for the study of RB and VBB removal by PTW

Model	Equation
Pseudo first order	$\frac{dq_t}{dt} = k_1 \cdot (q_e - q_t)$
Pseudo second order	$\frac{dq_t}{dt} = k_2(q_e - q_t)^2$
Elovich	$qt = \frac{1}{\beta} \cdot \ln(\alpha \cdot \beta) + \frac{1}{\beta} \cdot \ln(t)$

With: *q_t* adsorbed amount at given time *t* (mg/g), *k₁* pseudo first order model constant (min⁻¹), *k₂* second-order model constant (g/mg·min⁻¹), *q_e* equilibrium dye concentration on adsorbent (mg/g), *t* time (min), *α* Initial adsorption rate (mg/g), *β* Desorption constant (g/mg) during every one experiment.

The agreement between the measured and the calculated adsorbed amounts was determined according to the estimated values of the determination coefficients as well as the calculated average percentage errors (APE_{kin} (3)):

$$\text{APE}_{\text{kin}}(\%) = \frac{\sum_{i=1}^N |(q_{t,\text{exp}} - q_{t,\text{theo}})/q_{t,\text{exp}}|}{N} \times 100 \quad (3)$$

where *q_{t,exp}* and *q_{t,theo}* (mg·g⁻¹) are the measured and the theoretical adsorbed amounts at the time “*t*”, *N* is the number of experiments.

2.3.3. Effect of initial dye concentrations—isortherm study

The effect of the initial dyes concentrations on their removal by the PTW was assessed at equilibrium for a contact time of 3 h, a pH of 4 and an adsorbent dose of 0.1 g·L⁻¹. The tested dye concentrations were adjusted to 10, 20, 30, 40 and 50 mg·L⁻¹ in single mode and 6, 8, 10, 12 and 14 mg·L⁻¹ in binary mode. The measured data were fitted to well-known models (Table 2), namely Freundlich, Langmuir and Temkin models. The original and linearized equations of these models as well as the assumptions and implications have been intensively developed in the literature [47,48].

As for the kinetic study, the concordance between the experimental and predicted adsorbed amounts

Table 2. Used isotherms models for the study of RB and VBB removal by PTW

Models	Equations
Langmuir	$q_e = \frac{q_m \cdot K_L \cdot C_e^{\frac{1}{n}}}{1 + K_L \cdot C_e}$
Freundlich	$q_e = K_f \cdot C_e^{\frac{1}{n}}$
Temkin	$q_e = B_L \cdot \ln(K_t) + B_L \cdot \ln(C_e)$

by the three used models was determined as follows (4):

$$\text{APE}_{\text{isotherm}}(\%) = \frac{\sum_1^N |(q_{t,\text{exp}} - q_{t,\text{theo}}) / q_{t,\text{exp}}|}{N} \times 100 \quad (4)$$

where $q_{e,\text{exp}}$ and $q_{e,\text{theo}}$ ($\text{mg} \cdot \text{g}^{-1}$) are the measured and the theoretical adsorbed dyes quantities at equilibrium.

2.3.4. Effect of adsorbent dose

The effect of the adsorbent dosage on the RB and VBB removal efficiency was determined for contact times ranging between 0 and 40 min, at initial dye concentrations of $10 \text{ mg} \cdot \text{L}^{-1}$ in single and binary modes. The PTW tested doses were equal to 0.05; 0.1; 0.15, and $0.2 \text{ g} \cdot \text{L}^{-1}$. The dye percentage removal for a given dose and time is calculated using (2).

2.3.5. Effect of temperature—thermodynamic study

The effect of the temperature on RB and VBB removal efficiency was determined for a fixed contact time of 3 h, and an initial dye concentration of $10 \text{ mg} \cdot \text{L}^{-1}$ in single and binary modes. The tested temperatures were fixed to 20, 30, 40, 50, and 60°C , at a constant adsorbent dosage of $0.1 \text{ g} \cdot \text{L}^{-1}$ and a fixed pH of 4 for both RB and VBB. The dye percentage removal for a given dose and time are calculated using (2).

The thermodynamic parameters of dyes adsorption onto the tested material have concerned the standard free energy changes ΔG° ($\text{kJ} \cdot \text{mol}^{-1}$), the enthalpy ΔH° ($\text{kJ} \cdot \text{mol}^{-1}$) and entropy changes ΔS°

($\text{kJ} \cdot \text{mol}^{-1} \cdot \text{K}^{-1}$). These parameters were calculated according to the following equations:

$$\Delta G^\circ = -RT \log K_C \quad (5)$$

$$\Delta G^\circ = \Delta H^\circ - T \Delta S^\circ \quad (6)$$

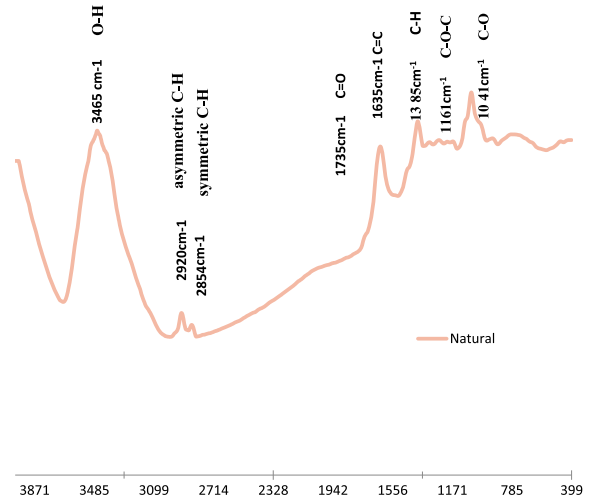
$$K_C = \frac{q_e}{C_e} \quad (7)$$

where R is the gas universal gas constant ($8.31 \text{ J} \cdot \text{K}^{-1} \cdot \text{mol}^{-1}$), T is the temperature (K) and K_C is the distribution coefficient.

The Van't Hoff equation can be deduced from the combination of (5) and (6) as follows:

$$\log K_C = \frac{\Delta S^\circ}{R} - \frac{\Delta H^\circ}{RT} \quad (8)$$

The Van't Hoff plot ($\log(K_C)$ as a function of $1/T$) permits the estimation of ΔH° and ΔS° through the calculus of its slope and intercept, respectively.

**Figure 2.** FTIR spectrum of the petiole palm tree waste.

3. Results and discussion

3.1. Adsorbent characterization

The pH_{PZC} value of the used adsorbent was found to be 3.8. According to the literature, values of 5.1, 6.13 and 6.5 were found in the case of the pH_{PZC} studies for mixture palm waste (seeds, leaves and bark) [49], date stone [43] and palm bark powder [50] respectively.

Therefore, the adsorbent's surface should be negatively charged for pH values higher than 3.8 which will favor the removal of the used cationic dyes. At

contrarily, for pH lower than 3.8, the solid surface should be positively charged.

On the other hand, the FTIR analysis of the used adsorbent (Figure 2) showed that this material contains various absorption peaks, which are characteristic of a lingo-cellulosic material [51].

The main existing bands were distributed as follows: (i) a broad and intense band around 3465 cm^{-1} corresponding to O–H bands [52], (ii) bands at 2920 cm^{-1} and 2854 cm^{-1} , that can be attributed to asymmetric C–H and symmetric C–H bands respectively [53], (iii) a band around 1735 cm^{-1} representing C=O and stretching vibration of ester group in hemicellulose [54], (iv) a band around 1635 cm^{-1} , showing the existence of C=C [55], (v) a band around 1635 cm^{-1} representing O–H bending of adsorbed water [55], and (vi) two bands around 1161 cm^{-1} and 1041 cm^{-1} attributed to the C–O–C asymmetric stretching vibration and C–O stretching ring in cellulose and hemicellulose, respectively [53].

The PTW's FTIR spectrum confirm the results of Belela *et al.* [56] who studied MB bio-sorption from aqueous solutions by date stones and palm-tree wastes. This spectrum confirmed that the PTW had various functional groups that would contribute to the VBB and RB removal from aqueous solutions.

3.2. Adsorption studies

3.2.1. Effect of initial pH

The value of pH_{PZC} indicated the type of active sites and biomass adsorption capacity. At a $\text{pH} > \text{pH}_{\text{PZC}}$, cationic dye adsorption was promoted, owing to the presence of functional groups such as OH[−] and COO[−] groups, whereas at a $\text{pH} < \text{pH}_{\text{PZC}}$, anionic dye adsorption was promoted, here the surface became positively charged [57].

The effect of the pH values on VBB and RB adsorption was studied under the experimental conditions in Section 2.3.1. It can be seen that the adsorption of the two dyes is influenced by the solutions pH values (Figure 3). Indeed, the lowest adsorption yields for VBB (20.2%) and RB (70.2%) were obtained for the lowest pH value (3). This may be due mainly to the fact at this pH, the adsorbent was mainly positively charged which induces a net reduction of the adsorption of the positively charged

studied dyes. When used pH values are higher than the pH_{PZC} , the adsorption yields of both dyes increase. The corresponding average yields values for this range were assessed to 26%, and 79.6%, for VBB and RB, respectively. The highest adsorption yields were determined at a pH of 4. They were assessed to 85.4% and 35.2% for RB and VBB, respectively. Kataria *et al.* [58] observed that the maximum removal of Victoria blue b dye was achieved at pH 6, after that, it decreased with increase in pH when Al-Gheethi *et al.* [59] observed that the maximum removal of Rhodamine B dye was achieved at pH 4.69.

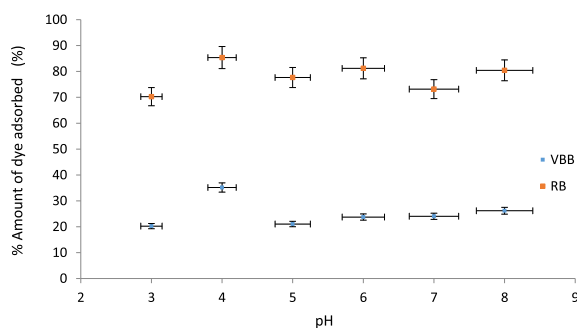


Figure 3. Effect of pH on the adsorption of VBB and RB by PTW (Concentration = $20\text{ mg}\cdot\text{L}^{-1}$, contact time = 3 h and adsorbent dose = 0.1 g).

3.2.2. Adsorption kinetics

The adsorption kinetic of VBB and RB by PTW was carried out under the experimental conditions given in Figure 4. It can be clearly seen that this process is time and initial concentration dependent. Indeed, for a given constant initial concentration, the adsorbed dye amount in both modes highly increases at the beginning of the experiment until a contact time of 15 min. At this time duration, for a single mode and at a concentration of $50\text{ mg}\cdot\text{L}^{-1}$, the VBB and RB adsorbed amounts represented about 47%, and 31% of the totally adsorbed amount at the end of the experiment. This short duration will be particularly appreciated when this process will be scaled up for real applications since it will permit high energy savings. After this duration, the VBB and RB adsorption continue to increase but with a much slower rate (Figure 4). After a longer contact period, the adsorbed amounts continue to increase but at a slower rate. This behavior can be

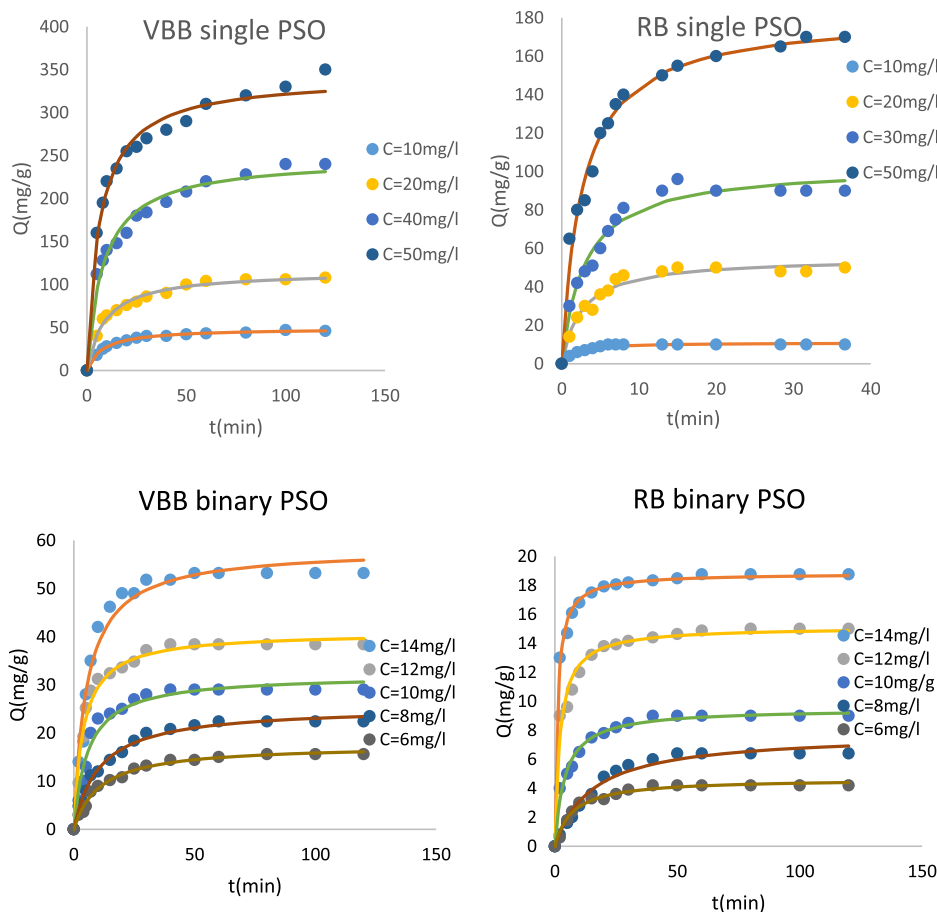


Figure 4. RB and VBB kinetic removal by the petiole palm waste at different initial concentrations in single and binary systems.

linked to intra-particle diffusion within the adsorbent pores and dye adsorption [60,61]. The equilibrium state which corresponds to almost constant adsorbed amounts was reached after a longer contact time. However, in all cases, duration of about 120 min was sufficient to reach this equilibrium state.

It is important to underline that the equilibrium time increases with the increase of the initial dye concentration. For example, in a single mode, for an initial concentration of $10 \text{ mg}\cdot\text{L}^{-1}$, this time was assessed to 6 and 15 min for RB and VBB, respectively. These times increased to 20 and 60 min when the used initial dyes concentration was increased to $50 \text{ mg}\cdot\text{L}^{-1}$. This behavior is mainly due to the fact that higher is the initial dye concentration, higher are the dyes molecules that will react with fixed adsorption sites on the surface of PTW [62]. Similar trend was observed for the binary mode (Figure 4).

The increase of the adsorbed dyes amount in single and binary systems with the increase of the initial concentration will be deeply discussed in the isotherm section (Section 3.2.3). Moreover, the dyes removal efficiency decrease in binary mode in comparison with the single system will be examined in the same Section 3.2.3.

The fitting of the experimental data with the PFO, PSO, and Elovich kinetic models shows that the PSO was the best one. Indeed, the corresponding theoretical adsorption data for the two dyes and the two studied modes are more concordant with the experimental data in comparison with the other models. The PSO model exhibited the highest average calculated R^2 (0.979) and the lowest APE (5.33%) (Table 3). This result suggests that the dyes removal by PTW might mainly a chemical process including complexation with the adsorbent functional groups and cation exchange [63,64].

Table 3. Parameters of the kinetics models of the adsorption of RB, and VBB by PTW in single and binary modes at different initials concentrations (contact time = 3 h, pH = 4 and adsorbent dose = 0.1 g.L⁻¹)

Dyes	Pseudo first order model				Pseudo second order model				Elovich model				
	C0 (mg/l)	q_e (mg/g)	k_1 (min ⁻¹)	R^2	APE	k_2 (10 ⁻³ min ⁻¹)	q_e (mg/g)	R^2	APE	α	$1/\beta$	R^2	APE
Rhodamine B, single mode	10	10.09	0.447	0.991	2.686	65.47	10.96	0.965	5.749	66.92	1.505	0.725	10.737
	20	49.31	0.280	0.980	5.643	6.996	55.23	0.969	5.605	65.7	9.945	0.870	10.035
	30	91.46	0.249	0.975	6.443	3.269	103	0.967	6.355	103.5	18.87	0.889	8.446
	50	161.9	0.272	0.926	7.023	2.068	181.7	0.984	4.227	231.6	31.92	0.958	5.183
		Average		0.968	5.448			0.971	5.484			0.860	8.600
Victoria Blue B, single mode	10	43.58	0.094	0.980	4.653	2.549	49.23	0.996	1.877	21.54	8.572	0.952	4.507
	20	101.6	0.083	0.956	7.628	0.948	115.5	0.988	3.611	39.43	20.96	0.970	3.769
	40	218.9	0.088	0.923	9.829	0.480	247.6	0.977	5.316	105.4	43	0.991	1.874
	50	305.4	0.114	0.935	7.864	0.456	342.1	0.982	3.679	250.5	54.366	0.987	2.122
		Average	0.948	7.493			0.983	3.620			0.975	3.068	
Rhodamine B, binary mode	14	18.03	0.505	0.963	4.599	49.85	18.83	0.995	1.317	6248	1.516	0.867	3.118
	12	14.28	0.264	0.923	7.134	31.35	15.13	0.977	3.510	221.2	1.641	0.916	3.858
	10	8.76	0.156	0.955	6.763	26.05	9.496	0.984	3.924	15.74	1.361	0.916	5.840
	8	6.545	0.059	0.995	4.124	8.524	7.785	0.977	9.303	1.15	1.633	0.935	13.425
	6	4.142	0.107	0.982	6.330	30.62	4.653	0.981	8.647	1.778	0.863	0.900	14.318
	Average		0.963	5.79				0.982	5.34			0.906	8.111
Victoria Blue B, binary mode	14	52.71	0.142	0.991	3.945	3.282	58.34	0.974	6.756	38.27	9.85	0.849	13.300
	12	37.42	0.184	0.979	5.226	6.303	40.92	0.979	6.275	52.29	6.209	0.839	12.519
	10	28.78	0.132	0.985	5.120	5.383	32.08	0.969	9.097	16.37	5.681	0.854	15.587
	8	22.12	0.078	0.986	6.234	3.751	25.47	0.989	5.966	5.94	5.025	0.955	8.334
	6	15.16	0.077	0.984	6.758	5.13	17.55	0.989	6.342	3.851	3.516	0.959	11.631
	Average		0.985	5.456			0.98	6.887				0.891	12.274

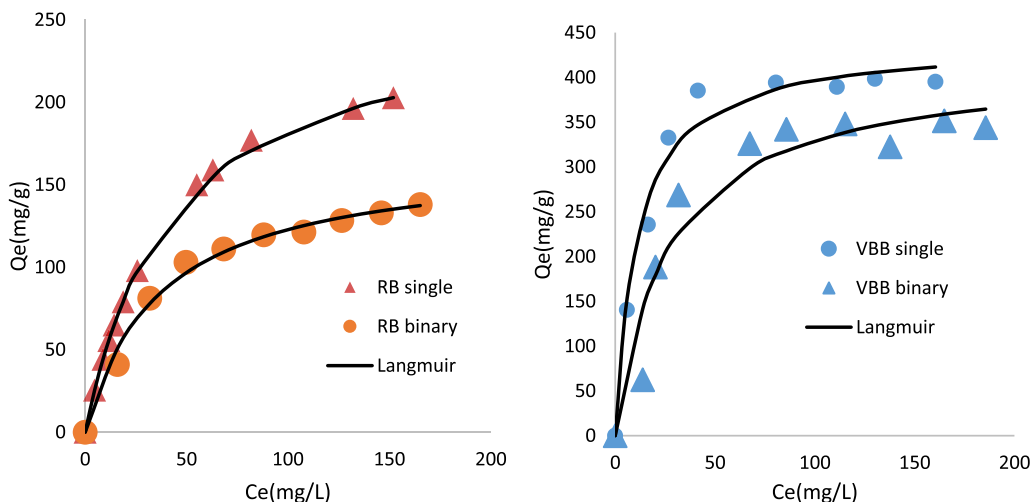


Figure 5. Isothermal experimental and fitted data with, Langmuir model for RB and VBB removal by PTW in single and binary mode (initial pH = 4; adsorbent dosage = $0.1 \text{ g} \cdot \text{L}^{-1}$; contact time = 3 h; $T = 20 \pm 2 \text{ }^{\circ}\text{C}$).

Table 4. Calculated parameters of Langmuir, Freundlich and Temkin models regarding RB and VBB removal by TPW in single and binary mode

Dye	Langmuir				Freundlich				Temkin			
	K_L (L/mg)	Q_m (mg/g)	R^2	APE (%)	K_f (L/mg)	n	R^2	APE (%)	B (J/mol)	K_t	R^2	APE (%)
Rhodamine B, single mode	0.023	260.1	0.992	7.3	18.17	2.0	0.9587	20.4	56	0.243	0.982	6.9
Victoria Blue B, single mode	0.089	440.1	0.948	5.9	136.6	4.4	0.9183	13.3	77.32	1.63	0.864	10.1
Rhodamine B, binary mode	0.027	168	0.977	4.6	21.43	2.6	0.9137	9.1	38.86	0.227	0.968	5.6
Victoria Blue B, binary mode	0.037	417.4	0.860	20.1	71.73	3.1	0.7346	26.9	93.54	0.313	0.817	21.9

Similar results were reported in various research studies, namely the adsorption of methylene blue and crystal violet by palm kernel fiber [65] and the adsorption of Dye Basic Blue 41 and Basic Yellow 28 by activated carbon [66].

3.2.3. Effect of dyes initial concentration—isootherm study

The impact of the initial dyes concentrations in single and binary modes on their removal by PTW was evaluated under the experimental conditions given in Section 2.3.3. The used pH was fixed to 4

which correspond to the optimal value found in Section 3.2.1. The measured data as well as the theoretical ones calculated by Langmuir, Freundlich and Temkin models are given in Figure 5. The calculated constants of these three models are given in Table 4.

On the basis of Figure 5 and Table 4, it can be clearly deduced that the adsorbed amounts of RB and VBB in single mode were higher than the ones observed in binary system. Indeed, in single mode, the palm tree waste exhibited an uptake capacity of 440.1 , and $260.1 \text{ mg} \cdot \text{g}^{-1}$ for VBB and

Table 5. Comparison of RB and VBB adsorption onto PTW with other materials

Adsorbent	Dye	Langmuir's adsorption capacity, q_m , (mg·g ⁻¹)	Reference
Seed husk of Bengal gram	RB, single mode	133.34	[67]
Ordered mesoporous carbon material ST-A	RB, single mode	83	[68]
Commercial adsorbent (activated carbon CWZ-22)	RB, single mode	58	[68]
Synthesized hybrid ion exchanger	RB, single mode	76.4	[69]
Montmorillonite/graphene oxide nanocomposite	RB, binary mode	178.6	[70]
Organo-vermiculites	RB, binary mode	261.97	[71]
Surfactant-modified three-dimensional Mg Al layered double hydroxide	RB, binary mode	49.6	[72]
Flower shaped Zinc 5 oxide nanoparticles	VBB, single mode	163.93	[58]
Incense stick ash	VBB, single mode	77.67	[73]
PTW	RB, single mode	260.1	Present work
	VBB, single mode	440.1	
PTW	RB, binary mode	168	Present work
	VBB, binary mode	417.4	

RB, respectively. These adsorption capacities diminished by 35.4%, and 5.2%, respectively in binary mode. This finding is mainly due to a competitive adsorption between the two dyes on the available adsorption sites [66,74,75]. On the other hand, the confrontation of the experimental data to the three used isotherm models showed that the Langmuir model was the most suitable one with relatively high correlation coefficients and lower APE (Table 4). In addition, the highest Langmuir's parameter values " $R_L = 1/(1 + K_L \cdot C_0)$ " were estimated to 0.483 and 0.218 for RB and VBB in single mode 0.448 and 0.38 in binary mode. All these values are less than 1 which indicates that the two dyes adsorption by PTW is a favorable process. This result suggests that dyes adsorption onto PTW occurs on uniform monolayer coverage at the outer surface of the adsorbents [76]. On the other hand, under the studied conditions, the Freundlich parameter " n " varied between 2.2 and 4.4. They are in the range of 1–10, which suggests that the adsorption of these two dyes by the PTW is a favorable process. Values in the same range were determined by [77], and [78]

when studying RB, and VBB removal by graphene-based nickel nano-composite, and activated carbon, Ba/alginate and modified carbon/Ba/alginate polymer beads, respectively.

Temkin model was also tested, under the studied conditions, The Temkin parameter " B " varied between 38.86 and 93.54 J/mol, these values are less than 8 kJ/mol which implies that the biosorption of the two dyes is physical in the simple binary system [79,80].

In order to situate our adsorbent efficiency in removing the studied dyes, we made a comparison of its removal efficiency (based on the Langmuir's adsorption capacity) with several other raw and modified adsorbents (Table 5). Results indicate that the PTW could be considered as an attractive low cost material for dyes removal from aqueous solutions. In fact, the adsorption capacity of the RB studied during this work in single mode was about 260.1 mg/g, this value is higher than results found by other researchers we quote for example 133.34 mg/g, 83 mg/g, 76.4 mg/g, and 58 mg/g.

Table 6. Effect of temperature on RB and VBB adsorption onto PTW

	T (°C)	Q_m (mg/g)	ΔG° (kJ·mol ⁻¹)	ΔH° (kJ·mol ⁻¹)	ΔS° (J·mol ⁻¹ ·K ⁻¹)
Rhodamine B, single mode	20	260.1	-25.744	-11.312	49.107
	30	249.1	-26.251		
	40	258.8	-26.608		
	50	224.1	-27.0615		
	60	211	-27.814		
Victoria Blue B, single mode	20	440.1	-27.681	-9.740	62.515
	30	439.8	-29.110		
	40	414	-29.606		
	50	327.9	-29.823		
	60	313.5	-30.385		
Rhodamine B, binary mode	20	168	-24.591	-17.277	25.858
	30	168.3	-25.177		
	40	163.8	-25.714		
	50	149.5	-26.087		
	60	101.3	-25.341		
Victoria Blue B binary mode	20	417.4	-26.801	-16.518	35.832
	30	368.9	-27.666		
	40	322.1	-27.716		
	50	290	-28.334		
	60	227.6	-28.215		

3.2.4. Effect of adsorbent dose

The PTW mass effect on the dye was studied in single and binary systems under the experimental conditions given in Section 2.3.4. Results (Figure 6) indicated that the two dyes uptake yields increased with increasing the PTW doses. For instance, at a fixed time (25 min), increasing the dose of the adsorbent from 0.05 g/L to 0.2 g/L, increased the removal yields from about 6% to 24%, 40% to 81%, 24% to 40% and 6% to 13% for RB and VBB in single mode and for VBB and RB in binary system, respectively. This finding is mainly due to the increase of the available adsorption active sites that could react with the dyes molecules. Similar results were reported by [81,82], and [83] when studying the adsorption of lead (Pb(II)) from aqueous solutions by Lignite, five toxic dyes by industrial graphite, and cationic crystal violet dye by graham flour.

3.2.5. Effect of temperature

The experimental results of the dye adsorption in single and binary systems on PTW are shown in Figure 7 and Table 6.

On the basis of Figure 7 and Table 6, it appears that for all studied cases, the increase of the temperature has resulted in a decrease of the adsorbed amounts. Indeed, when rising temperature from 20 to 60 °C, the RB and VBB adsorbed amounts decreased by about 39.06%, and 34.84% in single mode and by 53.68%, and 55.77% in binary system.

The thermodynamic parameters of the studied cases are given in Table 6, the thermodynamic energy calculation showed that the studied biosorption is physical (ΔH less than 40 kJ/mol), spontaneous, and exothermic ($\Delta H < 0$) with an increase in disorder ($\Delta S > 0$) [84]. Similar results was observed by [85] and [86] when studying adsorption of Rhodamine-

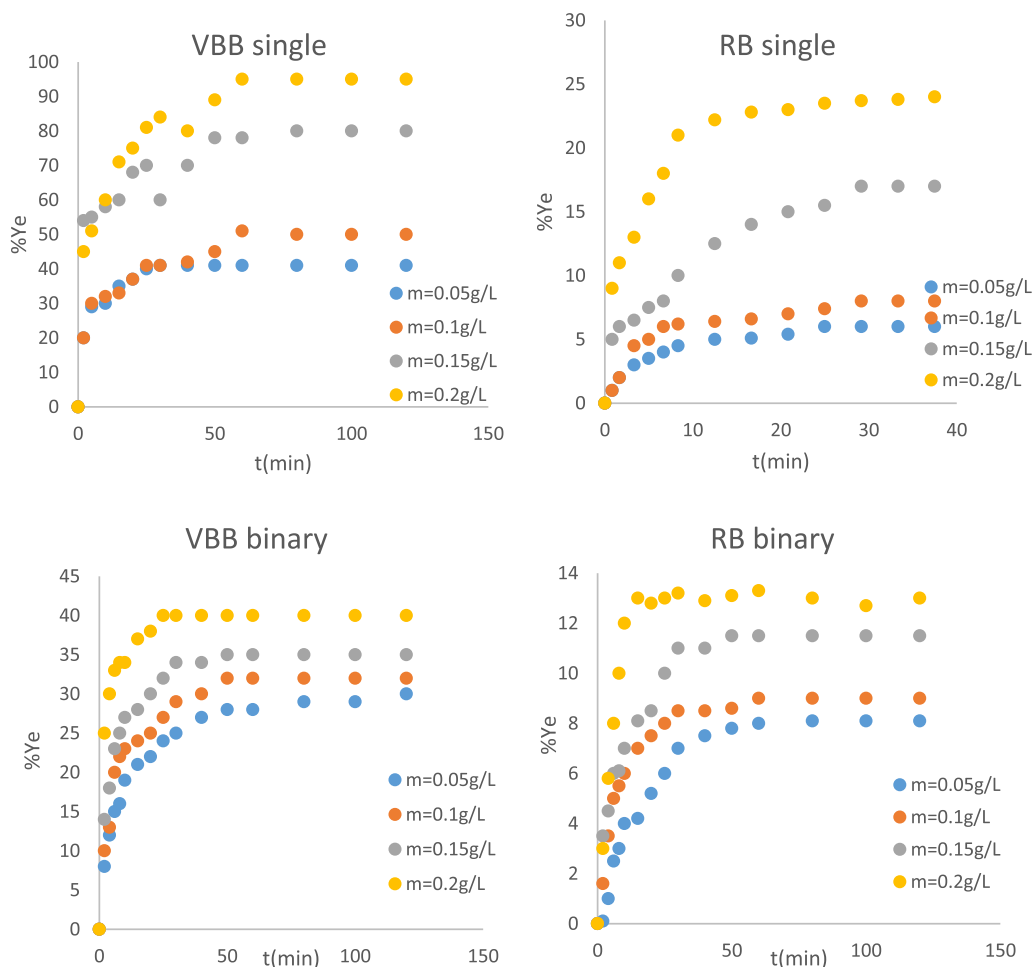


Figure 6. Effect of PTW doses on the removal yield of RB and VBB in single and binary systems.

B from aqueous solution by the use of natural adsorbent perlite and magnetic silica nanocomposite immobilized *Pseudomonas fluorescens* respectively, while [87] observed that the removal of RB from aqueous solutions using MgO supported Fe-Co-Mn nano-particles was spontaneity and endothermic similar results was observed by [58] when studying the adsorption of VBB onto zinc oxide nanoparticles.

4. Mechanisms exploration

To remove contaminants from an aqueous solution, it is necessary to understand the mechanism of the solute adsorption onto the solid surface. During

an adsorption mechanism there is intervention of ionic interactions of opposite charge namely dipole-dipole, dipole-induced dipole, hydrogen bonding, chemical bonding and ion exchange.

In order to interpret the adsorption of the solute, the adsorbent surface chemistry as well as its effect on the adsorption process is usually studied. Fourier transform infrared spectroscopy (FTIR) analysis is used to study the interaction between an adsorbate and the active sites on the adsorbent surface. The explanation of FTIR is based on the chemical structure of petiole palm tree wastes. PTW consists mainly of three compounds which are cellulose, hemicellulose and lignin. Cellulose and hemicellulose contain most of the oxygenated functional

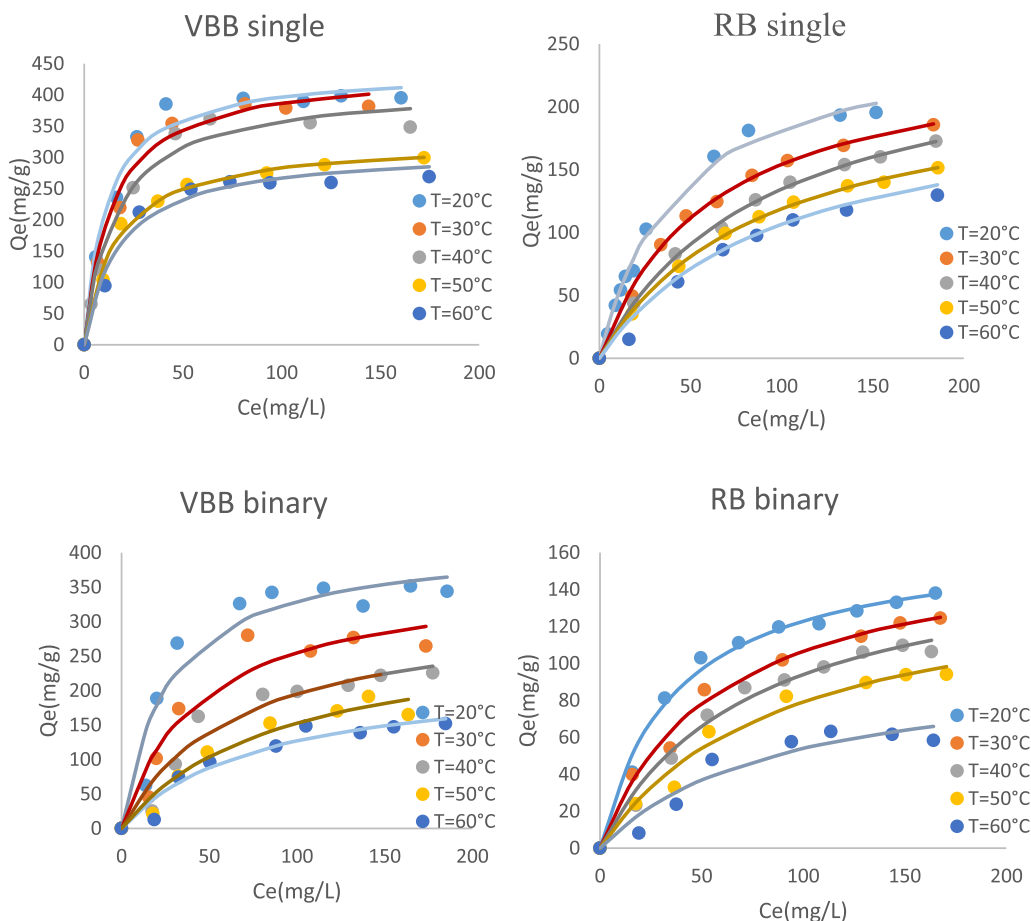


Figure 7. Effect of temperature on the adsorption of RB and VBB in single and binary system.

groups present in the lignocellulose product, while lignin is a complex, systematically polymerized and highly aromatic substance [38].

5. Conclusions

Rhodamine B (RB) and Victoria blue B (VBB) dye removal from aqueous solutions in single and heterogeneous solutions using petiole palm tree waste (PPTW) was experimentally determined.

Our findings were:

- In the single system:

The removal percentage increased with increasing initial dye concentration and adsorbent mass and decreased with increasing temperature. Langmuir and Freundlich's models described the adsorption isotherms well but Langmuir's model fitted

better the experimental data with adsorption capacities of 260.1 and 440.1 mg/g for RB and VBB, respectively. The thermodynamic energy calculation showed that the studied biosorption is physical, spontaneous, and exothermic with an increase in disorder. Concerning the kinetic study, the optimum contact time for the initial dye concentration to reach equilibrium is 60 min and 20 min for (VBB) and (RBB), respectively. This result is due to the saturation of active sites. The experimental results showed that the chemical adsorption best followed the pseudo-second-order equation.

- In the binary system:

The removal percentage increased with the initial dye concentration and adsorbent mass but decreased with increasing temperature. In contrast to the other tested models, the Langmuir model fitted

the experimental data better with adsorption capacities, calculated from the linear Langmuir equation, equal to 168 and 417.4 mg/g for RB and VBB, respectively. The optimum contact time for the initial dye concentration to reach equilibrium was 40 and 20 min for VBB and RBB, respectively. This result is attributable to the negatively charged surface area. The adsorption curve followed the Pseudo-second order model.

Conflicts of interest

Authors have no conflict of interest to declare.

Acknowledgments

The authors would like to thank the National Engineering School of Gabes, Gabes University, Tunisia. Special thanks to Mrs. Rim Najjar for many helpful style corrections.

References

- [1] G. Thompson, J. Swain, M. Kay, C. Forster, *Bioresour. Technol.*, 2020, **77**, 275-286.
- [2] S. Gopi, A. Pius, S. Thomas, *J. Water Process. Eng.*, 2016, **14**, 1-8.
- [3] V. Hernández-Montoya, M. A. Pérez-Cruz, D. I. Mendoza-Castillo, M. R. Moreno-Virgen, A. Bonilla-Petriciolet, *J. Environ. Manage.*, 2013, **116**, 213-221.
- [4] S. T. Akar, A. S. Özcan, T. Akar, A. Özcan, Z. Kaynak, *Desalination*, 2009, **249**, 757-761.
- [5] M. Singh, H. S. Dosanjh, H. Singh, *J. Water Process. Eng.*, 2016, **11**, 152-154.
- [6] S. Guiza, L. Franck, M. Bagané, *Desalination Water Treat.*, 2018, **113**, article no. 22258.
- [7] P. N. Tim Robinson, G. McMullan, R. Marchant, *Bioresour. Technol.*, 2001, **77**, 247-255.
- [8] R. Ahmad, *J. Hazard. Mater.*, 2009, **171**, 767-773.
- [9] A. M. Salah, D. K. Mahmoud, W. A. W. A. Karim, A. Idris, *A Compr. Rev.*, 2011, **280**, 1-13.
- [10] B. H. U. G. Akpan, *J. Hazard. Mater.*, 2009, **170**, 520-529.
- [11] A. K. Verma, R. R. Dash, P. Bhunia, *J. Environ. Manage.*, 2012, **93**, 154-168.
- [12] A. A. Azzaz, S. Jellali, H. Akrou, A. A. Assadi, L. Bousselmi, *J. Clean. Prod.*, 2018, **201**, 28-38.
- [13] L. B. Ahmed Amine Azzaz, A. Amine Assadi, S. Jellali, A. Bouzaza, D. Wolbert, S. Rtimi, *J. Photochem. Photobiol. A*, 2018, 111-120, [Online].
- [14] V. Vijayakumar, R. Saravanathamizhan, N. Balasubramanian, *J. Water Process. Eng.*, 2016, **9**, 155-157.
- [15] S. Cheng, D. L. Oatley, P. M. Williams, C. J. Wright, *Water Res.*, 2011, **46**, 33-42.
- [16] Y. Cui, Q. Ge, X. Liu, T. Chung, *J. Membr. Sci.*, 2014, **467**, 188-194.
- [17] M. Khan, I. M. C. Lo, *Water Res.*, 2016, **106**, 259-271.
- [18] S. Jellali, B. Khiari, M. Usman, H. Hamdi, Y. Charabi, M. Jeguirim, *Renew. Sust. Energy Rev.*, 2021, **144**, article no. 111068.
- [19] A. Hammami, C. Charcosset, R. Ben, *J. Membr. Sci. Technol.*, 2017, **7**, 1-8.
- [20] P. Velmurugan, V. Rathina Kumar, G. Dhinakaran, *Int. J. Environ. Sci.*, 2011, **1**, 1492-1503.
- [21] S. Guiza, M. Bagane, *J. Water Sci.*, 2013, **26**, 39-51.
- [22] S. Guiza, M. Bagane, *J. Univ. Chem. Technol. Metall.*, 2012, **47**, 283-288.
- [23] G. Mezohegyi, F. P. van der Zee, J. Font, A. Fortuny, A. Fabregat, *J. Environ. Manage.*, 2012, **102**, 148-164.
- [24] X. L. W. Wang, G. Huang, C. An, X. Xin, Y. Zhang, *Appl. Surf. Sci.*, 2017, **405**, 119-128.
- [25] M. Boutaieb, M. Guiza, S. Román, B. Ledesma Cano, S. Nogales, A. Ouederni, *C. R. Chim.*, 2020, **15**, 607-621, [Online].
- [26] Suhas, V. K. Gupta, P. J. M. Carrott, R. Singh, M. Chaudhary, S. Kushwaha, *Bioresour. Technol.*, 2016, **216**, 1066-1076.
- [27] H. Naeem, H. N. Batti, S. Sadaf, M. Iqbal, *Appl. Radiat. Isot.*, 2017, **123**, 94-101.
- [28] J. Luan, P. X. Hou, C. Liu, C. Shi, G. X. Li, H. M. Cheng, *J. Mater. Chem.*, 2016, **4**, 1191-1194.
- [29] L. R. Bonetto, F. Ferrarini, C. de Marco, J. S. Crespo, R. Guégan, M. Giovanela, *J. Water Process. Eng.*, 2015, **6**, 11-20.
- [30] M. Akram, H. N. Batti, M. Iqbal, S. Noreen, S. Sadaf, *J. Environ. Chem. Eng.*, 2017, **5**, 400-411.
- [31] Y. Safa, H. N. Bhatti, M. Sultan, S. Sadaf, *Desalination Water Treat.*, 2016, **57**, 25532-25541.
- [32] S. Sadaf, H. Bhatti, *Desalination Water Treat.*, 2016, **57**, 11773-11781.
- [33] S. Sadaf, H. N. Bhatti, S. Nausheen, M. Amin, *J. Taiwan Inst. Chem. Eng.*, 2015, **47**, 160-170.
- [34] A. A. Azzaz, S. Jellali, R. Souissi, K. Ergaieg, L. Bousselmi, *Environ. Sci. Pollut. Res.*, 2017, **24**, 18240-18256.
- [35] S. Kuppusammy, K. Venkateswarlu, Y. B. L. P. Thvamani, R. Naidu, M. Megharaj, *Ecol. Eng.*, 2017, **101**, 3-8.
- [36] N. Boudouaia, Z. Bengharez, S. Jellali, *Appl. Water Sci.*, 2019, **9**, 1-12.
- [37] N. El Kadri, M. Ben Mimoun, J. I. Hormaza, *Sci. Hortic. (Amsterdam)*, 2019, **253**, 24-34.
- [38] T. Ahmad *et al.*, *Environ. Sci. Pollut. Res.*, 2012, **19**, 1464-1484.
- [39] I. A. W. Tan, B. H. Hameed, A. L. Ahmad, *Chem. Eng. J.*, 2007, **127**, 111-119.
- [40] S. Montoya-Suarez, F. Colpas-Castillo, E. Meza-Fuentes, J. Rodríguez-Ruiz, R. Fernandez-Maestre, *Water Sci. Technol.*, 2015, **37**, 21-27.
- [41] M. Wakkal, B. Khiari, F. Zagrouba, *C. R. Chim.*, 2020, **23**, 671-687.
- [42] A. A. Azzaz, S. Jellali, M. Jeguirim, L. Bousselmi, Z. Bengharez, H. Akrou, *C. R. Chim.*, 2021, **21**, 71-84.
- [43] H. Hammami, M. El Achaby, K. El Harfi, M. A. El Mhammedi, *C. R. Chim.*, 2020, 589-606.
- [44] S. Guiza, *Ecol. Eng.*, 2017, **99**, 134-140.
- [45] C. Chakrapani, C. S. Babu, K. N. K. Vani, K. S. Rao, *E-J. Chem.*, 2010, **7**, 419-427.

- [46] M. Firdaus, M. Yusop, M. A. Ahmad, N. A. Rosli, M. Edeerozey, A. Manaf, *Arab. J. Chem.*, 2021, **14**, 103-122.
- [47] D. Suteu, T. Malutan, D. Bilba, *Desalination*, 2010, **255**, 84-90.
- [48] A. Ergene, K. Ada, S. Tan, H. Kat, *Desalination*, 2009, **249**, 1308-1314.
- [49] K. Azoulay, I. Bencheikh, A. Moufti, A. Dahchour, J. Mabrouki, S. El Hajjaji, *Chem. Data Collect.*, 2020, **27**, 1-29.
- [50] Z. Chaouki, M. Hadri, M. Nawdali, M. Benzina, H. Zaitan, *Sci. Afr.*, 2021, **12**, 1-16.
- [51] C. Xu et al., *Sci. Total Environ.*, 2021, **790**, article no. 148089.
- [52] K. Kanjana, P. Harding, T. Kwamman, W. Kingkam, *Biomass Bioenergy*, 2021, **153**, article no. 106206.
- [53] H. Boumediri, A. Bezazi, G. G. Del Pino, A. Haddad, F. Scarpa, A. Dufresne, *Carbohydr. Polym.*, 2019, **222**, article no. 114997.
- [54] C. B. T. L. Lee, T. Y. Wu, C. K. Cheng, L. F. Siow, I. M. L. Chew, *Ind. Crops Prod.*, 2021, **166**, article no. 113397.
- [55] Y. Zhao et al., *Ind. Crops Prod.*, 2015, **65**, 96-101.
- [56] Z. Belala, M. Jeguirim, M. Belhachemi, F. Addoun, G. Trouvé, *Desalination*, 2011, **271**, 80-87.
- [57] R. Chikri, N. Elhadiri, M. Benchanaa, Y. El, *J. Chem.*, 2020, **11**, 1-17.
- [58] N. Kataria, V. K. Garg, M. Jain, K. Kadirvelu, *Adv. Powder Technol.*, 2016, **27**, 1180-1188.
- [59] A. A. Al-gheethi et al., *Chemosphere*, 2022, **287**, article no. 132080.
- [60] J. Huang, K. Huang, S. Liu, A. Wang, C. Yan, *Colloids Surf. A Physicochem. Eng. Asp. J.*, 2008, **330**, 55-61.
- [61] M. Haneda, H. Hamada, *C. R. Chim.*, 2021, **15**, 1-12, [Online].
- [62] N. KhaledMahmoudi, M. Hamdia, S. Ben Alia, Jellalic, E. Srasraa, *C. R. Chim.*, 2020, **23**, 689-704.
- [63] C. Duan, T. Ma, J. Wang, Y. Zhou, *J. Water Process. Eng.*, 2020, **37**, 101-339.
- [64] S. Jellali, A. A. Azzaz, M. Jeguirim, H. Hamdi, A. Mlayah, *Water (Switzerland)*, 2021, **13**, 1-19.
- [65] G. O. El-Sayed, *Desalination*, 2011, **272**, 225-232.
- [66] A. Regti, A. El Kassimi, M. R. Laamari, *J. Assoc. Arab Univ. Basic Appl. Sci.*, 2016, **24**, 1-9.
- [67] M. C. Somasekhara Reddy, V. Nirmala, *Arab. J. Chem.*, 2017, **10**, S2406-S2416.
- [68] K. Jedynak, D. Wideł, R. Nina, *Colloids Interfaces*, 2019, **17**, 1-16.
- [69] Saruchi, V. Kumar, *Arab. J. Chem.*, 2019, **12**, 316-329.
- [70] M. Neelaveni, P. Santhana Krishnan, R. Ramya, G. Sonia Theres, K. Shanthi, *Adv. Powder Technol.*, 2019, **30**, 596-609.
- [71] M. Yu, M. Gao, T. Shen, H. Zeng, *J. Mol. Liq.*, 2019, **292**, article no. 111408.
- [72] Z. Zhu, M. Xiang, P. Li, L. Shan, P. Zhang, *J. Solid State Chem.*, 2020, **288**, article no. 121448.
- [73] S. N. Jain, S. R. Tamboli, D. S. Sutar, V. N. Mawal, A. A. Shaikh, A. A. Prajapati, *Sustain. Chem. Pharm.*, 2020, **15**, article no. 100199.
- [74] Y. Al-Degs, M. A. M. Khraisheh, S. J. Allen, M. N. Ahmad, G. M. Walker, *Chem. Eng. J.*, 2007, **128**, 163-167.
- [75] M. A. Wahab, R. Ben Hassine, S. Jellali, *J. Hazard. Mater.*, 2011, **191**, 333-341.
- [76] S. Liu, *J. Colloid Interface Sci.*, 2015, **450**, 224-238.
- [77] U. Jinendra, D. Bilehal, B. M. Nagabhushana, A. Praveen, *Helvion*, 2021, **7**, article no. e06851.
- [78] M. Kumar, R. Tamilarasan, V. Sivakumar, *Carbohydr. Polym.*, 2013, **98**, 505-513.
- [79] R. Maryanti, A. B. D. Nandiyanto, T. I. B. Manullang, A. Hufad, Sunardi, *Sains Malays.*, 2020, **49**, 2977-2988.
- [80] N. Ayawei, A. N. Ebelegi, D. Wankasi, *J. Chem.*, 2017, **2017**, 1-11.
- [81] M. Haneda, H. Hamada, *C. R. Chim.*, 2016, **15**, 1-12, [Online].
- [82] S. Ambika, V. Srilekha, *Environ. Adv.*, 2021, **4**, article no. 100072.
- [83] K. T. Kubra, M. S. Salman, H. Znad, M. N. Hasan, *J. Mol. Liq.*, 2021, **329**, article no. 115541.
- [84] A. Ausavasukhi, C. Kampoosaen, O. Kengnok, *J. Clean. Prod.*, 2016, **134**, 506-514.
- [85] R. T. M. Dharmendirakumar, G. Vijayakumar, G. Vijayakumar, R. Tamilarasan, M. Dharmendirakumar, *J. Mater. Environ. Sci.*, 2015, **3**, 157-170.
- [86] G. J. Joshiba, P. S. Kumar, M. Govarthan, P. T. Nueagni, A. Abilarasu, F. Carolin, *Environ. Pollut.*, 2021, **269**, article no. 116173.
- [87] S. Rahdar, A. Rahdar, M. Nadeem, *J. Mater. Technol.*, 2019, **8**, 3800-3810.